EMBO reports

scientific report

Structural and functional analysis of the putative pH sensor in the Kir1.1 (ROMK) potassium channel

Markus Rapedius[1], Shozeb Haider[2]*, Katharine F. Browne[3], Lijun Shang[3], Mark S.P. Sansom[2], Thomas Baukrowitz[1]+ & Stephen J. Tucker[3]++*

[1]Institute of Physiology II, Friedrich Schiller University, Jena, Germany, [2]Structural Bioinformatics and Computational Biochemistry Unit, Department of Biochemistry, and [3]Oxford Centre for Gene Function, Department of Physiology, Anatomy and Genetics, University of Oxford, Oxford, UK

The pH-sensitive renal potassium channel Kir1.1 is important for K^+ homeostasis. Disruption of the pH-sensing mechanism causes type II Bartter syndrome. The pH sensor is thought to be an anomalously titrated lysine residue (K80) that interacts with two arginine residues as part of an 'RKR triad'. We show that a Kir1.1 orthologue from *Fugu rubripes* lacks this lysine and yet is still highly pH sensitive, indicating that K80 is not the H^+ sensor. Instead, K80 functionally interacts with A177 on transmembrane domain 2 at the 'helix-bundle crossing' and controls the ability of pH-dependent conformational changes to induce pore closure. Although not required for pH inhibition, K80 is indispensable for the coupling of pH gating to the extracellular K^+ concentration, explaining its conservation in most Kir1.1 orthologues. Furthermore, we demonstrate that instead of interacting with K80, the RKR arginine residues form highly conserved inter- and intra-subunit interactions that are important for Kir channel gating and influence pH sensitivity indirectly.

Keywords: ROMK; Kir1.1; potassium channel; Bartter syndrome
EMBO reports (2006) **7**, 611–616. doi:10.1038/sj.embor.7400678

INTRODUCTION

Kir1.1 (ROMK) is a member of the inwardly rectifying (Kir) family of potassium channels, characterized by its sensitivity to intracellular pH (pH_i) in the physiological range. Kir1.1 channels are found in the apical membrane of epithelial cells lining the distal nephron of the kidney, where they secrete excess K^+ into the urine and are therefore the principal regulators of K^+ homeostasis in the body. Their inhibition by H^+ has an important role, linking K^+ transport and electrical activity to cellular H^+ homeostasis (Schulte & Fakler, 2000; Hebert *et al*, 2005). Furthermore, inherited mutations in Kir1.1 that disrupt this pH-sensing mechanism hypersensitize the channel to H^+ and result in type II Bartter syndrome, a hypokalaemic disorder (Hebert, 2003).

The Kir1.1 pH sensor is thought to be a lysine residue (K80) at the base of the first transmembrane domain (TM1; Fakler *et al*, 1996). However, the pK_a of lysine in free solution is 10.5, and to function as a H^+ sensor at physiological pH it must show anomalous titration. Schulte *et al* (1999) proposed that two cytoplasmic arginine residues, R41 in the amino terminus and R311 in the carboxy terminus, interact with K80 in an 'RKR triad' to produce this anomalous titration and this hypothesis remains the accepted explanation for the pH sensitivity of Kir1.1.

However, mutations at this position in TM1 of Kir3.2 and Kir6.2 produce ligand-insensitive channels. But in both cases, these effects are explained by changes in their intrinsic gating properties, rather than by loss of ligand binding (Trapp *et al*, 1998; Yi *et al*, 2001; Wang *et al*, 2005). We therefore postulated that K80 may not be the actual H^+ sensor itself, but, instead, may form a crucial part of the Kir1.1 gating machinery, which transduces the response of the channel to pH_i into pore closure, and that mutations at K80 reduce ligand (i.e. H^+) efficacy through an indirect mechanism. Recent advances in structural biology now provide X-ray crystal structures of the cytoplasmic domains of two mammalian Kir channels (Kir2.1 and Kir3.1; Nishida & Mackinnon, 2002; Pegan *et al*, 2005) in addition to the complete structures of two prokaryotic Kir channels, KirBac1.1 (Kuo *et al*, 2003) and KirBac3.1 (Protein Data Bank (PDB) file 1XL6). This therefore presents an unparalleled opportunity to readdress the 'RKR triad' hypothesis.

In this study, we have used a combination of electrophysiology, homology modelling and molecular dynamics (MD) simulations to examine the structure of Kir1.1 and we present a new mechanistic and structural insight into the important role of these RKR residues in Kir channel gating, pH sensitivity and sensitivity to extracellular K^+.

[1]Institute of Physiology II, Friedrich Schiller University, Jena, Germany
[2]Structural Bioinformatics and Computational Biochemistry Unit, Department of Biochemistry, and [3]Oxford Centre for Gene Function, Department of Physiology, Anatomy and Genetics, University of Oxford, Oxford, UK
*These authors contributed equally to this work
+Corresponding author. Tel: +49 3641 938860; Fax: +49 3641 933202;
E-mail: thomas.baukrowitz@mti.uni-jena.de
++Corresponding author. Tel: +44 1865 272500; Fax: +44 1865 272469;
E-mail: stephen.tucker@physiol.ox.ac.uk

Received 7 December 2005; revised 20 January 2006; accepted 8 March 2006; published online 21 April 2006

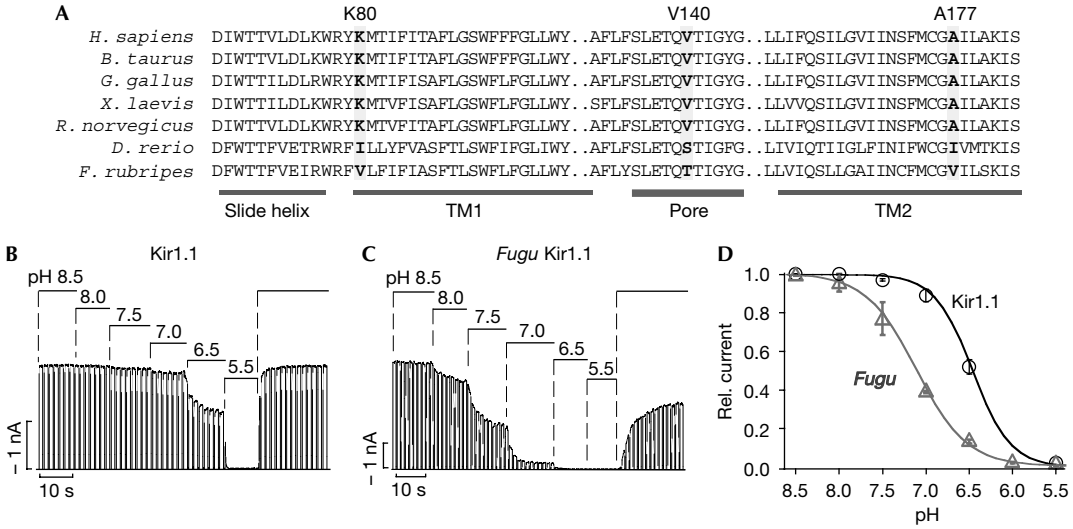

Fig 1 | *Fugu* Kir1.1 is pH sensitive without a lysine at position 80. (**A**) Partial alignment of *Fugu* Kir1.1 with rat Kir1.1 (residues 67–183) and other orthologues (see Methods) reveals that it lacks a lysine at position 80 (boxed grey). Other highlighted residues are V140 and A177, which are not conserved in the *Fugu* or zebrafish orthologues. (**B**) pH titration of Kir1.1 currents with pH solutions as indicated. Kir1.1 currents were recorded from giant inside-out patches evoked by voltage steps from −80 to +20 mV; only inward currents are shown. (**C**) pH titration of *Fugu* Kir1.1 currents; pH titrations were obtained subsequent to phosphatidylinositol 4,5-bisphosphate (PIP_2) application to establish stable channel activity; however, PIP_2 application did not affect the pH sensitivity (data not shown). (**D**) Normalized pH dose–response curves fitted to a standard Hill equation. Values are given in Table 1.

RESULTS AND DISCUSSION

Fugu Kir1.1 is pH sensitive without a 'pH sensor lysine'

We proposed that if the lysine residue in TM1 (K80) is the actual titratable H^+ sensor, then this residue would be conserved in Kir1.1 orthologues across the species. TBLASTN analysis using the rat Kir1.1a sequence showed that this lysine residue is highly conserved in most species (Fig 1A). However, a Kir1.1 orthologue in the *Fugu rubripes* (Japanese puffer fish) genome showed 75% homology and 55% identity at the amino-acid level with the rat Kir1.1 sequence, yet has a valine instead of a lysine residue at the relevant position in TM1. A similar orthologue exists in the *Danio rerio* (zebrafish) genome (Fig 1A). We therefore cloned the *Fugu* Kir1.1 gene and compared it with the rat Kir1.1a clone by expression in *Xenopus* oocytes. Unless otherwise stated, 'Kir1.1' hereafter refers to the rat Kir1.1a sequence and all the mutants tested were made in rat Kir1.1a. Fig 1B–D shows that despite the lack of a TM1 'pH sensor' lysine residue, the *Fugu* Kir1.1 channel still shows a steep pH-dependent inhibition in the physiological range (see also Table 1).

Modelling and molecular dynamics simulations of Kir1.1

The pH sensitivity of *Fugu* Kir1.1 directly challenges the original hypothesis that K80 is the actual H^+ sensor. We therefore used a combination of homology modelling and MD simulations to build a model of Kir1.1 based on the known Kir/KirBac structures (Fig 2A). Energy minimization and MD simulations over a 10 ns period were used to demonstrate the structural stability of the model (see the supplementary information online and supplementary Fig S1 online). The distances between the RKR residues were calculated during the last 8 ns of the simulation and show that both arginine residues (R41, R311) are >24 Å from K80 and

Table 1 | Mean values ± s.e.m. for pH dose–response curves fitted to standard Hill equation for WT and mutant Kir1.1 channels with half-maximal pH inhibition ($pH_{0.5}$), Hill coefficient (Hill) and number of experiments (*n*)

Channel	$pH_{0.5}$	Hill	*n*
Kir1.1 wild type	6.5 ± 0.1	2.0 ± 0.1	10
K80I	5.5 ± 0.1	1.7 ± 0.1	12
K80M	5.4 ± 0.1	1.6 ± 0.1	12
K80V	5.3 ± 0.1	1.8 ± 0.1	12
A177C	7.9 ± 0.1	2.9 ± 0.2	11
A177T	7.8 ± 0.1	2.2 ± 0.1	11
A177V	8.5 ± 0.1	1.7 ± 0.1	12
K80I/A177I	6.7 ± 0.2	1.2 ± 0.1	8
K80I/A177T	7.1 ± 0.1	1.2 ± 0.1	12
K80M/A177C	6.6 ± 0.1	1.1 ± 0.1	10
K80M/A177T	6.5 ± 0.2	0.8 ± 0.1	13
K80V/A177V	8.3 ± 0.1	1.8 ± 0.1	16
E302D	7.2 ± 0.1	2.2 ± 0.1	17
E302Q	8.8 ± 0.1	0.7 ± 0.1	13
R311W	9.2 ± 0.1	1.5 ± 0.1	9
E318D	6.3 ± 0.1	2.4 ± 0.2	6
Fugu_Kir1.1	7.3 ± 0.2	1.5 ± 0.3	8

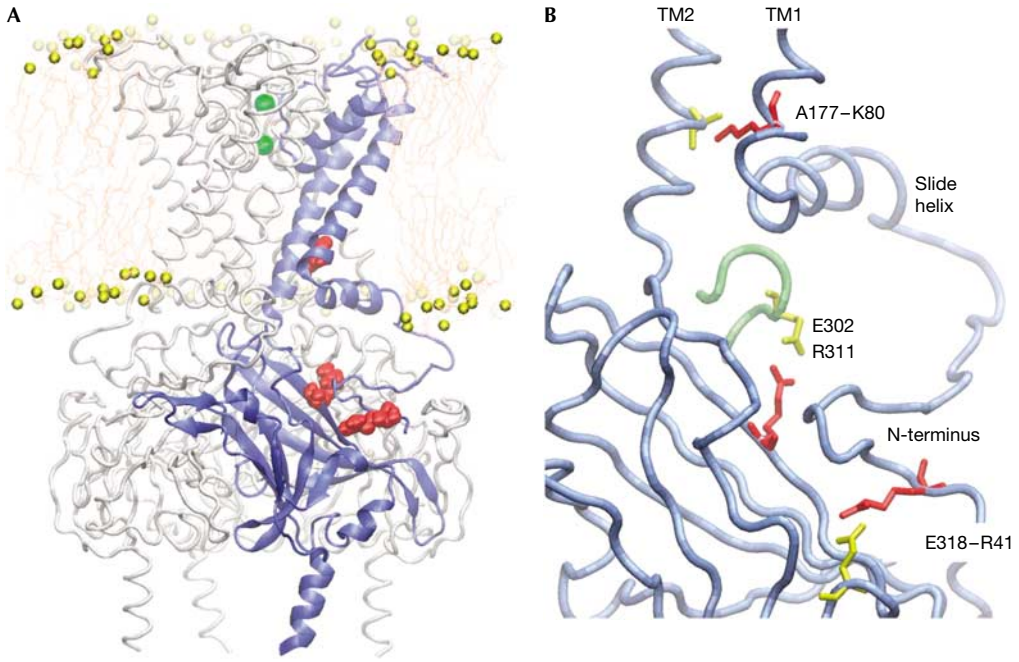

Fig 2 | Instead of interacting with each other, the 'RKR triad' residues form important inter- and intra-subunit interactions. (**A**) Side view of the structural model of tetrameric Kir1.1 channel (see Methods for details). One of the four subunits is coloured blue. The space-filled residues (red) correspond to the 'RKR triad' (R41–K80–R311). The lipid (POPC) bilayer is shown as yellow spheres and tails, whereas the K^+ ions in the selectivity filter are shown in green. K80 is >24 Å from both R41 and R311. Calculations of these distances are shown in greater detail in the supplementary information online (supplementary Figs S2,S3 online). (**B**) A single subunit of Kir1.1 is shown and coloured blue for clarity. R41, K80 and R311 are coloured red, whereas the residues they interact with (E318, A177, E302) are shown in yellow. The R41–E318 and K80–A177 interactions are intra-subunit. The R311–E302 interaction is inter-subunit and the relevant section of the adjacent carboxy terminus containing E302 is shown in green.

are therefore unlikely to influence the ionization state of K80 (supplementary Figs S2A,S3 online). We next calculated the solvent-accessible surface area of K80 during a 10 ns MD simulation. The results show that K80 is buried within the lipid membrane and remains completely inaccessible to solvent during the course of this simulation (supplementary information online and supplementary Fig S2B online). This residue is therefore likely to be in a predominantly unprotonated—that is, uncharged—form within the membrane.

RKR arginines form inter- and intra-subunit interactions

Instead of interacting with each other, R41 and R311 interact with highly conserved glutamate residues (Figs 2B,3). R41 in the amino-terminus of Kir1.1 forms a dynamically stable intra-subunit interaction with E318 in the carboxy-terminus (Figs 2B,3A; supplementary Fig S4 online). This salt bridge is also visible in KirBac3.1 (PDB file 1XL6) and these two residues are absolutely conserved in all 15 human Kir channels and in >50 other eukaryotic and prokaryotic Kir channel sequences (not shown), suggesting a highly conserved functional and/or structural role.

Charge reversal of this ion pair (R41E/E318R) produced nonfunctional channels (not shown). However, a more subtle mutation (E318D) caused a modest reduction in pH sensitivity ($pH_{0.5} = 6.3 \pm 0.1$; Fig 3B and Table 1). But more importantly, it also caused a profound difference in the ability of the channel to recover from pH inhibition; the activity of Kir1.1(E318D) showed only 13%±4% recovery, whereas wild-type channels showed 97%±1% recovery (Fig 3C,D). The mutational sensitivity of this interaction demonstrates that it has a crucial role in Kir channel structure and/or function.

The second RKR arginine (R311) also forms a dynamically stable inter-subunit ion pair with E302 on the adjacent C terminus (Figs 2B,3E; supplementary Figs S3,S4 online). These two residues are highly conserved across the species and their importance is highlighted by the fact that mutation of R311 in Kir1.1 causes Bartter syndrome (Schulte *et al*, 1999), whereas mutation of the equivalent glutamate (E303) in Kir2.1 causes Andersen's syndrome (Lopes *et al*, 2002). Charge reversal of this putative ion pair in Kir1.1 (E302R/R311E) produced nonfunctional channels (data not shown). However, the more subtle Kir1.1(E302D) mutation caused an alkaline $pH_{0.5}$ shift of approximately 0.5 units (Fig 3F and Table 1), whereas neutralization of this residue (E302Q) caused a substantial alkaline shift (Fig 3F and Table 1). As reported previously (Schulte *et al*, 1999), the Bartter syndrome mutation, Kir1.1(R311W), caused a comparable alkaline shift (Fig 3F), indicating that disruption of either residue in this putative ion pair has similar functional consequences. R311 has been implicated as a putative phosphatidylinositol 4,5-bisphosphate (PIP_2) interaction site in Kir2.1 channels (Lopes *et al*, 2002) and PIP_2 is a known activator of Kir1.1 channel activity. We therefore tested whether changes in PIP_2 affinity might underlie this observed shift in channel activity and pH sensitivity. However, even prolonged

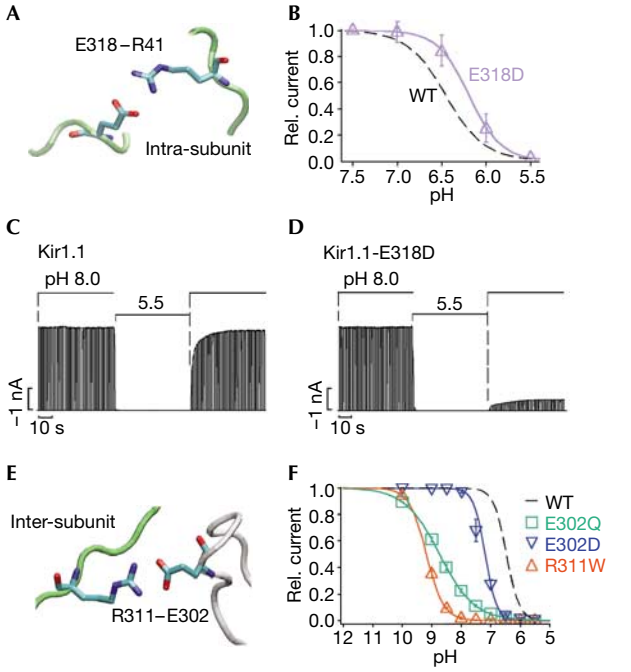

Fig 3 | Intra-subunit salt bridge R41–E318 and inter-subunit salt bridge R311–E302 affect pH gating in Kir1.1 channels. (**A**) Interaction between R41 (amino terminus) and E318 (carboxy terminus) magnified from the structural model shown in Fig 2B. Residues are coloured CPK. (**B**) Normalized pH dose–response curves for E318D (Table 1); the dotted line shows the wild type (WT) dose–response curve for comparison. (**C**) Kir1.1 channels recover completely from a pH inhibition (pH 5.5) lasting 45 s. (**D**) Kir1.1 E318D channels show little recovery from pH inhibition (pH 5.5). (**E**) Enlarged view of the interaction between R311 and E302. (**F**) Normalized pH dose–response curves for E302Q, E302D, R311W mutant and WT channels (values are given in Table 1).

exposure to PIP_2 (50 μM for 3 min) did not affect the pH inhibition of either wild-type or R311W channels, thus ruling out a PIP_2-related mechanism (not shown).

Control of pH gating at the helix-bundle crossing

Fig 4A demonstrates that mutation of K80 causes a significant shift, but not a complete loss, of Kir1.1 pH sensitivity; K80V, K80M and K80I all show a steep pH-dependent inhibition at low pH (Fig 4A,B). It is therefore unclear why *Fugu* Kir1.1 (with valine at position 80) is still strongly pH sensitive in the physiological range. However, examination of our model of Kir1.1 and MD simulations indicates that K80 forms a potential intra-subunit interaction with A177 <3 Å away on TM2 (Figs 2B,4C; supplementary Fig S4 online). Interestingly, both these residues occur at the transmembrane 'helix-bundle crossing' predicted to be an important part of the Kir channel gate (Kuo *et al*, 2003) and Fig 1A shows that *Fugu* Kir1.1 has a valine, not alanine, at position 177. Mutation of A177 causes an increase (i.e. alkaline shift) in pH sensitivity, whereas mutation of K80 causes a decrease in pH sensitivity (Fig 4B). Therefore, it is likely that it is the precise combination of residues at this position that is crucial for determining the response to pH_i. To test this, we made different combinations of mutations at K80 and A177 in Kir1.1; Fig 4B–D shows that, in nearly all cases, combining these mutations generated channels with a pH sensitivity similar to that of wild-type Kir1.1. This therefore explains why the *Fugu* Kir1.1 channel is still highly pH sensitive, even without a lysine in TM1; combining valine residues (as seen in *Fugu*; i.e. Kir1.1-K80V/A177V) or isoleucine residues (as seen in zebrafish) results in channels that are markedly more pH sensitive than the corresponding single mutations of K80 (Fig 4B–D and Table 1). Although the predicted proximity between K80 and A177, and the functional 'complementation' of mutations at these positions, is only suggestive of a direct physical interaction between them, the results clearly demonstrate the vital role of both transmembrane domains at the helix-bundle crossing in Kir channel gating and pH sensitivity.

To examine whether the pH-sensing mechanism in these double mutant channels remains similar to that of wild-type Kir1.1, we took advantage of the fact that Kir1.1 channels show state-dependent modification by the cysteine-reactive agent Cu-Phen (Cu(II)-1,10-phenanthroline); in wild-type Kir1.1, the pH-inhibited state is highly sensitive to Cu-Phen, whereas the open state is insensitive (Schulte *et al*, 1998). Kir1.1(K80I/A177T) exhibits the same closed-state-dependent modification as wild-type Kir1.1 (supplementary information online and supplementary Fig S5 online), indicating that the structural changes in the cytoplasmic domains required for pH-dependent inhibition of K80I/A177T channels are similar to those of wild-type Kir1.1, and strongly argues against their pH sensitivity being restored by an alternative mechanism.

Our results also explain why, in species that have a lysine at position 80, A177 is also conserved, and in orthologues that lack K80 (for example, *Fugu* and zebrafish) A177 is not conserved (Fig 1A). If this were not the case, then large shifts in pH sensitivity such as those seen would be observed with the individual mutations of K80 and A177, which would preclude pH regulation in the physiological pH range (Fig 4B–D).

Pathophysiology of the TM1–TM2 interaction

Interestingly, A177T is also a Bartter syndrome mutation, and the mechanism underlying this particular defect is not known (Peters *et al*, 2003). Fig 4B shows that A177T causes an alkaline shift in pH sensitivity ($pH_{0.5} = 7.8 \pm 0.1$; Table 1), thus explaining their loss of function at physiological pH. Intriguingly, K80 and A177 in Kir1.1 are also equivalent to residues T71 and C166 in the ATP-sensitive Kir channel, Kir6.2. Mutation of these residues in Kir6.2 causes a loss of ATP sensitivity (Trapp *et al*, 1998; Wang *et al*, 2005), with C166 mutations underlying a severe form of neonatal diabetes (DEND syndrome; Ashcroft, 2005). This demonstrates the importance of this intra-subunit 'helix-bundle crossing' interaction between TM1 and TM2 in defining the response of Kir channels to intracellular ligands and the pathophysiological consequences of disruption of this TM–TM interaction.

K80 controls the sensitivity to extracellular K^+

If K80 does not function as the actual H^+ sensor, then it is unclear why this residue is so highly conserved, except in *Fugu* and zebrafish. One possible reason is that Kir1.1 is normally sensitive to changes in extracellular K^+ concentrations; it is stimulated by extracellular K^+, whereas removal of extracellular K^+ causes irreversible loss of channel activity after pH inhibition. This property is thought to act as a positive feedback mechanism for

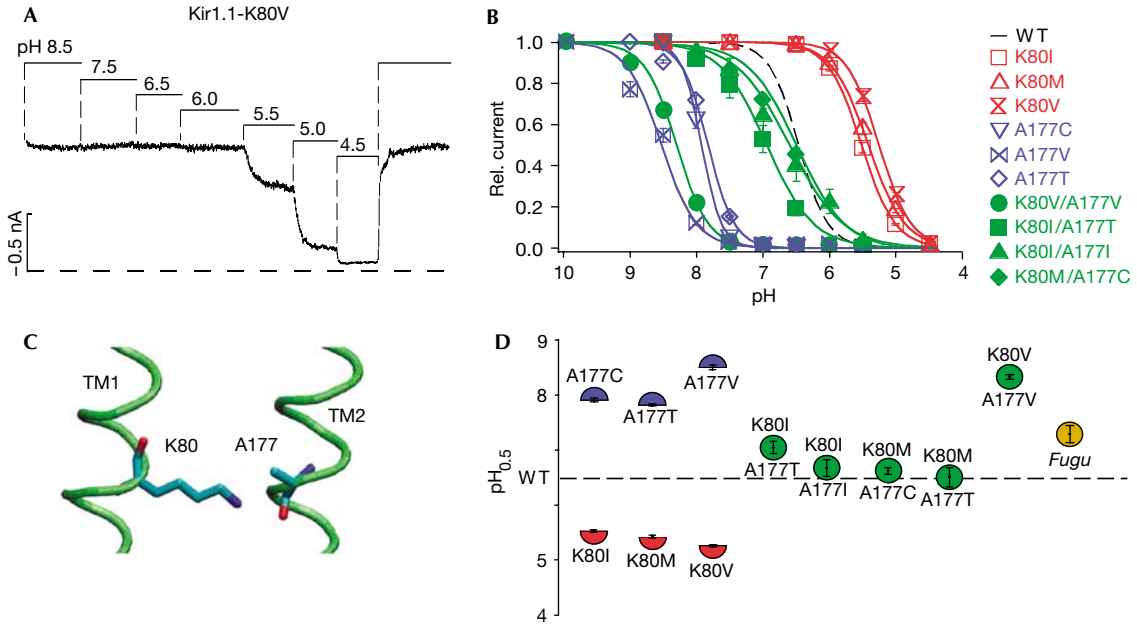

Fig 4 | K80–A177 interaction determines pH sensitivity of Kir1.1. (**A**) pH titration for K80V mutant channels, showing steep pH inhibition in the pH range 5.5–4.5. (**B**) Normalized dose–response curves for K80 mutant channels (red), A177 mutant channels (blue), K80/A177 mutant channels (green); values are given in Table 1. (**C**) Enlarged view of the interaction between K80 and A177. (**D**) Diagram showing the $pH_{0.5} \pm$s.e.m. values for the mutant channels depicted in (**B**) with the $pH_{0.5}$ for wild-type (WT) Kir1.1 channels shown as a dotted reference line and *Fugu* Kir1.1 shown in gold.

K^+ secretion and offers a unique tool with which to monitor the mechanism of coupling between pH inhibition and the extracellular K^+ sensor (Schulte & Fakler, 2000; Schulte *et al*, 2001; Dahlmann *et al*, 2004). Fig 5 shows that, like wild-type Kir1.1, A177T channels show no recovery after pH-induced inhibition in the absence of extracellular K^+. By contrast, the K80I/A177T and *Fugu* Kir1.1 channels lack this K^+ sensitivity and show almost full recovery. Thus, 'compensatory' mutations at positions 80/177 are able to restore 'normal' pH sensitivity, but do not restore sensitivity to extracellular K^+. These results demonstrate for the first time that the pH gating and extracellular K^+ gating mechanisms of Kir1.1 can be directly uncoupled, and illustrate the indispensable role of K80 in this K^+-sensing mechanism.

Furthermore, these results indicate that this crucial regulatory difference between *Fugu* Kir1.1 and Kir1.1 may reflect a different biological role for Kir1.1 orthologues in *Fugu* and other fishes. Although the pH sensitivity of *Fugu* Kir1.1 is conserved, indicating that it may have a physiological role, its sensitivity to extracellular K^+ is either not conserved or appeared later in evolutionary terms. Given the profoundly different renal structures and mechanisms of ion homeostasis used by fishes such as *Fugu* (Vize & Smith, 2004), it is likely that sensitivity to extracellular K^+ is not an important biological requirement for Kir1.1 orthologues in these organisms. Consistent with this hypothesis, the *Fugu* channel lacks a valine at position 140 in the pore helix (as does the zebrafish Kir1.1; Fig 1A), and previous studies have shown that Kir1.1 extracellular K^+ sensitivity is abolished by the V140T mutation (Schulte *et al*, 2001). Thus, the lack of sensitivity to extracellular K^+ seen in the *Fugu* Kir1.1 correlates with the absence of the physical structures known to be necessary for this property.

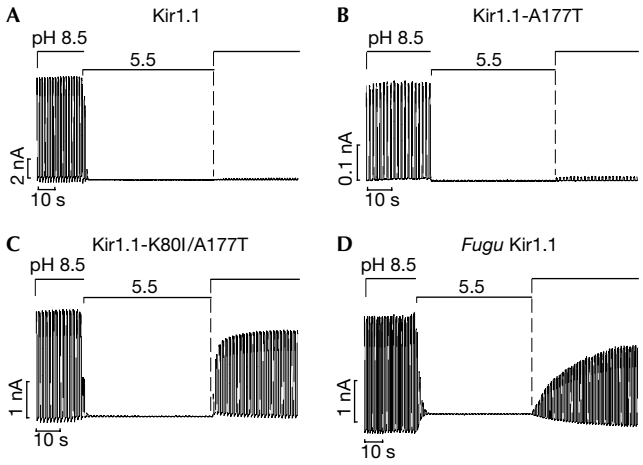

Fig 5 | K80 determines the sensitivity of Kir1.1 channels to extracellular K^+. Kir1.1 and mutant currents recorded in zero extracellular K^+. The pipette solution contained 120 mM *N*-methylglucamine instead of K^+ (K^+-free solution). Application of pH 8.5 and 5.5 solutions as indicated for (**A**) Kir1.1-WT, (**B**) Kir1.1-A177T, (**C**) Kir1.1-K80I/A177T and (**D**) *Fugu* Kir1.1 channels; similar results were obtained in $n > 3$ experiments for each mutant.

Conclusions

This study has built upon the important work by Schulte *et al* (1999) by providing a new mechanistic interpretation for the role of the RKR residues. Instead of forming a triad, the RKR arginine residues form highly conserved intra-subunit (R41:E318) and inter-subunit (R311:E302) interactions, both of which are fundamental

to Kir gating. Furthermore, instead of functioning as the H^+ sensor, K80 functionally interacts with A177 on TM2, and this intra-subunit interaction between the base of the transmembrane domains at the helix-bundle crossing is crucial for transducing the pH-dependent movement of the cytoplasmic domains into pore closure, an observation consistent with recent proposals that the pH-sensitive gate of Kir1.1 may reside at the base of TM2 (Sackin *et al*, 2005). The helix-bundle crossing is a highly conserved feature of K^+-channel pore architecture, and the interaction between K80 and A177 (i.e. TM1 and TM2) may be a feature common to the gating mechanism of K^+ channels in general. In addition, K80 is essential for coupling the pH gating of the channel to the response to extracellular K^+, a regulatory property not conserved in *Fugu* Kir1.1. Together, these 'RKR' residues, and the dynamic interactions that they control, present a new structural insight into a highly conserved Kir channel gating mechanism that has been adapted by Kir1.1 for the purpose of pH-dependent regulation and sensitivity to extracellular K^+.

METHODS

Molecular biology. Kir1.1 orthologues (XM_585917, XM_425795, BC074752, BC079788, NM_201035) were identified by TBLASTN analysis using the rat sequence (NM_017023) as a query. The *Fugu* orthologue was identified by searching the Fugu genome database (http://www.ensembl.org/Fugu_rubripes/index.html). The gene is encoded on a single exon and was isolated by PCR of genomic DNA. The sequence was verified by automated sequencing and deposited in GenBank (DQ279854). Kir1.1 subunits were subcloned into the oocyte expression vector pBF. 'Kir1.1' refers to the rat Kir1.1a sequence unless otherwise stated. Site-directed mutagenesis was performed using the QuikChangeII system (Stratagene, La Jolla, CA, USA). Messenger RNAs were synthesized *in vitro* by using the SP6 mMESSAGE mMACHINE kit (Ambion, Austin, TX, USA).

Model building. Homology models of Kir1.1 (residues 39–369) were generated using previous models of Kir6.2 as a structural template (Antcliff *et al*, 2005). MD simulations used GROMACS v3.1.4 (www.gromacs.org) and the GROMOS87 forcefield. pK_a values of individual residues in the model were calculated using the PropKa server (http://propka.chem.uiowa.edu/). The modelling and MD simulations are described in more detail in the supplementary information online.

Electrophysiology. *Xenopus* oocytes were manually defolliculated and injected with about 50 nl of mRNA. Giant patch recordings in inside-out configuration under voltage-clamp conditions were made at room temperature (21–25 °C) 3–7 days after mRNA injection. Pipettes had resistances of 0.3–0.9 MΩ (tip diameter 5–15 μm) and were filled with (in mM, pH adjusted to 7.2 with KOH) 120 KCl, 10 HEPES and 1.8 $CaCl_2$. K^+-free solution contained (in mM, pH adjusted to 7.2 with NaOH) 120 mM *N*-methylglucamine, 10 HEPES and 1.8 $CaCl_2$. Currents were sampled at 1 kHz with an analogue filter set to 3 kHz (−3 dB). Solutions were applied to the cytoplasmic side of excised patches via a multi-barrel pipette and had the following composition in mM (K_{int}): 120 KCl, 10 HEPES, 2 K_2EGTA and 1 Na Pyrophosphate, adjusted to appropriate pH level with HCl.

Supplementary information is available at *EMBO reports* online (http://www.emboreports.org).

ACKNOWLEDGEMENTS

We thank H. Fritzenschaft and S. Raabe for excellent technical assistance. This work was supported by the Wellcome Trust, the Royal Society and the Deutsche Forschungsgemeinschaft (Ba 1793/4-1). S.J.T. is a Royal Society University Research Fellow.

REFERENCES

Antcliff JF, Haider S, Proks P, Sansom MS, Ashcroft FM (2005) Functional analysis of a structural model of the ATP-binding site of the KATP channel Kir6.2 subunit. *EMBO J* **24:** 229–239

Ashcroft FM (2005) ATP-sensitive potassium channelopathies: focus on insulin secretion. *J Clin Invest* **115:** 2047–2058

Dahlmann A, Li M, Gao Z, McGarrigle D, Sackin H, Palmer LG (2004) Regulation of Kir channels by intracellular pH and extracellular K^+: mechanisms of coupling. *J Gen Physiol* **123:** 441–454

Fakler B, Schultz JH, Yang J, Schulte U, Brandle U, Zenner HP, Jan LY, Ruppersberg JP (1996) Identification of a titratable lysine residue thatdetermines sensitivity of kidney potassium channels (ROMK) to intracellular pH. *EMBO J* **15:** 4093–4099

Hebert SC (2003) Bartter syndrome. *Curr Opin Nephrol Hypertens* **12:** 527–532

Hebert SC, Desir G, Giebisch G, Wang W (2005) Molecular diversity and regulation of renal potassium channels. *Physiol Rev* **85:** 319–371

Kuo A, Gulbis JM, Antcliff JF, Rahman T, Lowe ED, Zimmer J, Cuthbertson J, Ashcroft FM, Ezaki T, Doyle DA (2003) Crystal structure of the potassium channel KirBac1.1 in the closed state. *Science* **300:** 1922–1926

Lopes CM, Zhang H, Rohacs T, Jin T, Yang J, Logothetis DE (2002) Alterations in conserved Kir channel–PIP2 interactions underlie channelopathies. *Neuron* **34:** 933–944

Nishida M, MacKinnon R (2002) Structural basis of inward rectification: cytoplasmic pore of the G protein-gated inward rectifier GIRK1 at 1.8 Å resolution. *Cell* **111:** 957–965

Pegan S, Arrabit C, Zhou W, Kwiatkowski W, Collins A, Slesinger P, Choe S (2005) Cytoplasmic domain structures of Kir2.1 and Kir3.1 show sites for modulating gating and rectification. *Nat Neurosci* **8:** 279–287

Peters M, Ermert S, Jeck N, Derst C, Pechmann U, Weber S, Schlingmann KP, Seyberth HW, Waldegger S, Konrad M (2003) Classification and rescue of ROMK mutations underlying hyperprostaglandin E syndrome/antenatal Bartter syndrome. *Kidney Int* **64:** 923–932

Sackin H, Nanazashvili M, Palmer LG, Krambis M, Walters DE (2005) Structural locus of the pH gate in the Kir1.1 inward rectifier channel. *Biophys J* **88:** 2597–2606

Schulte U, Fakler B (2000) Gating of inward-rectifier K^+ channels by intracellular pH. *Eur J Biochem* **267:** 5837–5841

Schulte U, Hahn H, Wiesinger H, Ruppersberg JP, Fakler B (1998) pH-dependent gating of ROMK (Kir1.1) channels involves conformational changes in both N and C termini. *J Biol Chem* **273:** 34575–34579

Schulte U, Hahn H, Konrad M, Jeck N, Derst C, Wild K, Weidemann S, Ruppersberg JP, Fakler B, Ludwig J (1999) pH gating of ROMK (Kir1.1) channels: control by an Arg–Lys–Arg triad disrupted in antenatal Bartter syndrome. *Proc Natl Acad Sci USA* **96:** 15298–15303

Schulte U, Weidemann S, Ludwig J, Ruppersberg J, Fakler B (2001) K^+-dependent gating of Kir1.1 channels is linked to pH gating through a conformational change in the pore. *J Physiol* **534:** 49–58

Trapp S, Proks P, Tucker SJ, Ashcroft FM (1998) Molecular analysis of ATP-sensitive K channel gating and implications for channel inhibition by ATP. *J Gen Physiol* **112:** 333–349

Vize PD, Smith HW (2004) A Homeric view of kidney evolution. *Anat Rec* **277A:** 344–354

Wang R, Rojas A, Wu J, Piao H, Adams CY, Xu H, Shi Y, Jiang C (2005) Determinant role of membrane helices in KATP channel gating. *J Memb Biol* **204:** 1–10

Yi BA, Lin YF, Jan YN, Jan LY (2001) Yeast screen for constitutively active mutant G protein-activated potassium channels. *Neuron* **29:** 657–667

SUPPLEMENTARY INFORMATION

Methods

Modelling and Molecular Dynamics Simulations

Homology models of Kir1.1 (residues 39-369) were generated using Modeller v7.0 [1]. Sequence alignments were done using ClustalX [2] with an identity of 45%. A four-fold symmetry option was imposed during the modelling procedure. An ensemble of 25 models were generated and the best model selected on the basis of low energy function and root mean square deviation (r.m.s.d.) from the template structure. The Cα-Cα r.m.s.d. between the template and the final selected model was 1.3Å. The quality and stereochemical properties of the models were evaluated using ProCheck v3.4.4 [3]. Molecular Dynamics simulations were carried out using GROMACS v3.1.4 [4] (www.gromacs.org) and the GROMOS87 forcefield [5].The protein molecule was embedded in Palmitoyl Oleoyl Phoshphatidyl Choline (POPC) bilayer using protocol that has been described in detail by Faraldo-Gomez *et al*. [6]. High-resolution X-ray studies of K^+ channels have revealed a vertical alignment of cationic charged ions in the filter region interspaced with solvent molecules (water). Positively charged K^+ ions were positioned in the selectivity filter by using crystallographically determined distances (7,8). The system is then solvated with SPC waters (9) in a box of size $14nm^3$. Additional counterions were added such that the overall net charge on the system is zero. The final system consisted of ~100000 atoms. The protein-lipid bilayer system was subjected to molecular mechanics energy minimisation with 1000 iterations of steepest descents. This is followed by the molecular dynamics equilibration step (0.30 ns) during which the protein atoms were restrained using a force constant of 1000 kJ/mol/nm^2. During this equilibration process, the water molecules and the ions are free to move. The final production simulation run was carried out on the system without any restraints for 10ns.

The parameters employed to undertake simulation used Berendsen coupling (10) to maintain a constant temperature of 300K and a constant pressure of 1 bar. Van der Waal's interactions were modelled using 6-12 Lennard Jones potential with a cutoff value of 1.2nm. Particle Mesh Ewalds

method (11,12) was employed to carry out long range electrostatic interactions with a cutoff of 1.2nm. LINCS algorithm (13) was employed to constrain the covalent bonds. The time step was 2fs and the coordinates saved after every 10ps for analysis. Analysis of the simulations was carried out using various programs in the present within the GROMACS suite of molecular dynamics packages. Structural diagrams were generated using VMD (14) and PyMol (www.pymol.org).

1. Sali A and Blundell TL (1993) *J. Mol. Biol.* **234**: 779-815.
2. Jeanmougin F, Thompson JD, Gouy M, Higgins DG, Gibson TJ. (1998) *Trends Biochem Sci*. **23**: 403-5.
3. Morris AL, MacArthur MW, Hutchinson EG, Thornton JM. (1992) *Proteins*. **12**: 345-64.
4. Berendsen HJC, van der Spoel D, van Drunen R. (1995) *Comput. Phys. Comm.* **95**: 43-56
5. van Gunsteren WF and Berendsen HJC. (1987) *Gromos87 Manual*, (Biomos BV, Groningen, The Netherlands)
6. Faraldo-Gomez JD, Smith GR and Sansom MS. (2002) *Eur Biophys J.* 31: 217-27.
7. Morais-Cabral JH, Zhou Y and MacKinnon R. (2001) *Nature*. 414: 37-42
8. Zhou Y, Morais-Cabral JH, Kaufman A, MacKinnon R. (2001) *Nature* 414: 43-8.
9. Berendsen HJC, Postma JPM, van Gunsteren WF, Hermans J. (1981) *Intermolecular forces* (Reidel, Dordercht, The Netherlands)
10. Berendsen HJC, Postma JPM, van Gunsteren WF, Dinola A, Haak JR. (1984) *J.Chem Phys.* 81:3684-3690
11. Darden T, York D., Pedersen L. (1993) *J. Chem. Phys* 98: 10089-10092
12. Essmann U, Perera L, Berkowitz ML, Darden T, Lee H, Pedersen L. (1995) *J Chem. Phys*. 103:8577-8593
13. Hess B, Bekker H, Berendsen HJC, Fraaije JGEM. (1997) *J.Comput.Chem.* 18: 1463-1472
14. Humphrey W, Dalke A, Schulten K. (1996) *J Mol Graph*. 14: 33-8, 27-8.

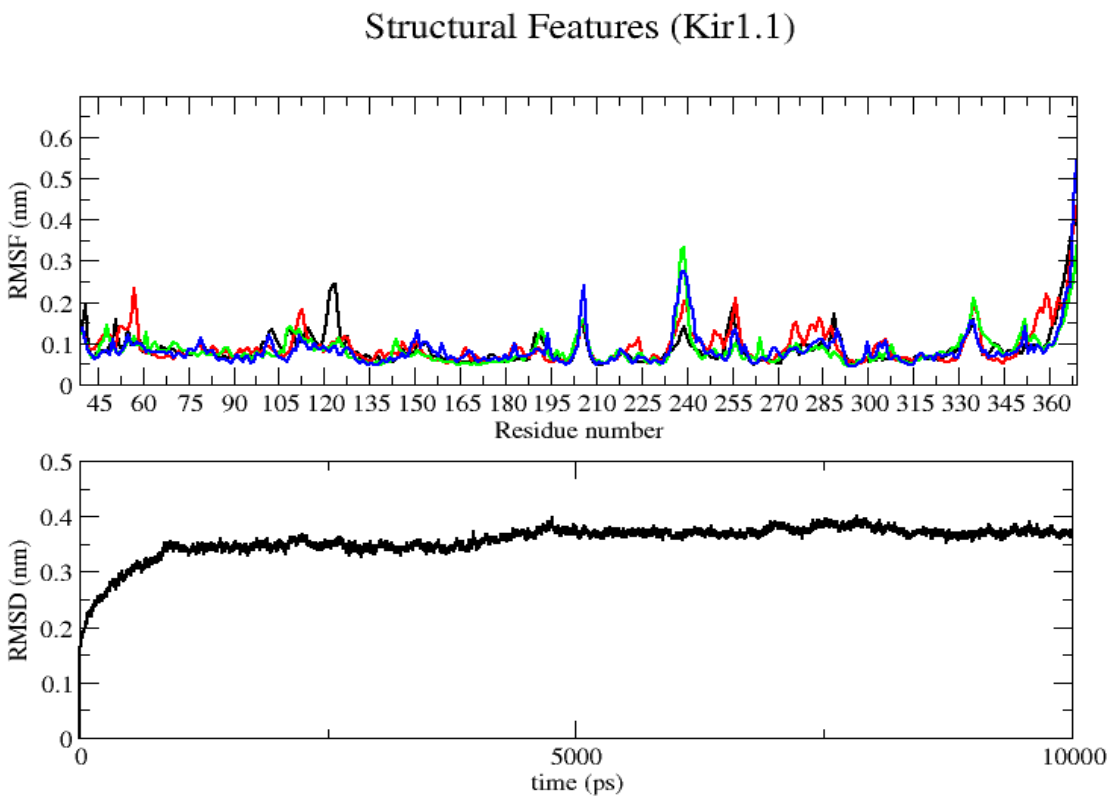

Supplementary Figure S1:

Upper Panel: Cα root mean square fluctuation (RMSF) plotted verses residue number. Each of the four subunits are represented in different colours. High fluctuating peaks on the plot correspond to loop regions within the structure.

Lower panel: Cα root mean square deviation (RMSD) for all residues of Kir1.1 tetramer plotted versus simulation time. The overall RMSD for the 10ns simulation is 3.5Å. These plots demonstrate the structural stability of the model over the entire 10000ps simulation run.

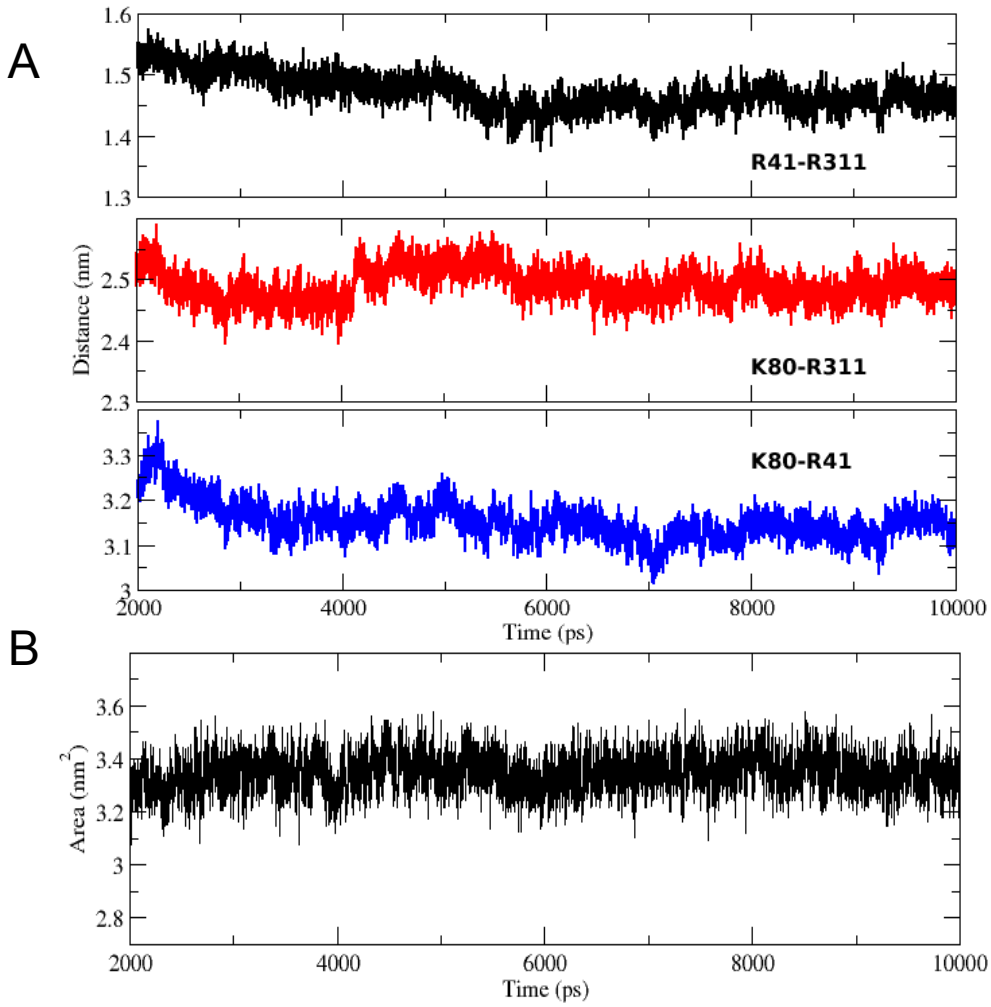

Supplementary Figure S2:

A. Calculated distances between 'RKR Triad' residues. This figure illustrates the averaged distance between individual residues of the putative 'RKR Triad' calculated over the final 8000ps molecular dynamics simulation. The average distances are : K80-R41 (blue) = 31.5Å, R41-R311 (black) = 14.71Å and R311-K80 (red) = 24.8Å.

B. K80 and A177 are solvent inaccessible. Solvent accessible surface area of K80-A177 interaction calculated over the 10000ps simulation run. The initial 2000ps (0-2000ps) have been treated as equilibration step and omitted. The final 8000ps have been used in the calculations using the g_sas program from the GROMACS suite of packages. K80 and A177 are located within the membrane and remain inaccessible to solvent over the entire course of the simulation.

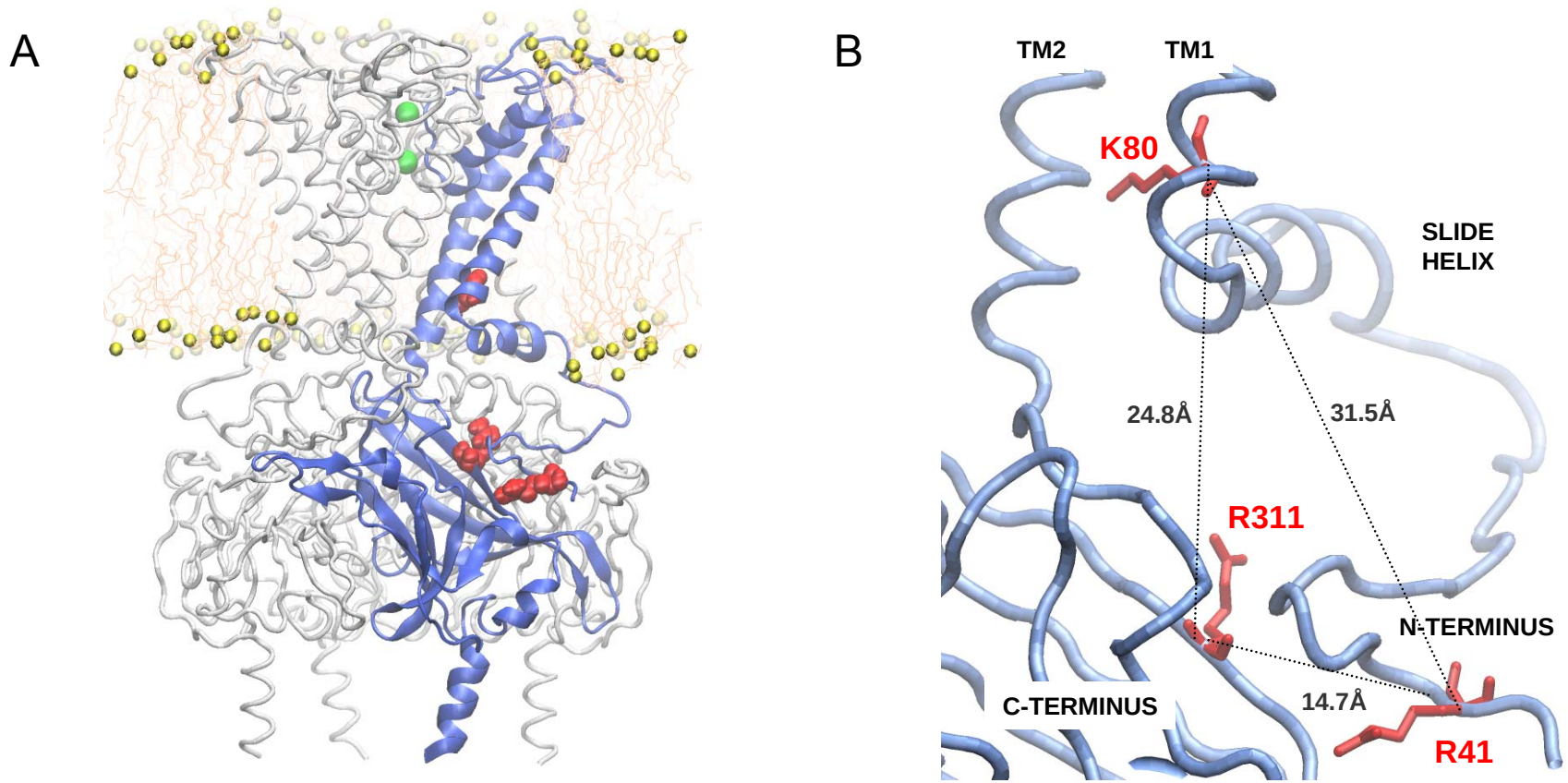

Supplementary Figure S3.

Model of Kir1.1 exposes the distance between the RKR Triad. A) Side view of the structural model of tetrameric Kir1.1 channel to illustrate the relative position of the RKR residues (red) within the tetramer. One of the four subunits is coloured blue. The lipid (POPC) bilayer is shown as yellow spheres and tails whilst the K^+ ions in the selectivity filter are shown in green. B) An expanded view of a single subunit of Kir1.1 is shown and coloured blue for clarity. The RKR residues (R41, K80, R311) are labelled red. The dotted lines and distances shown correspond to the Cα-Cα distance between them as averaged over an 8ns MD simulation (supplementary Fig. S2A).

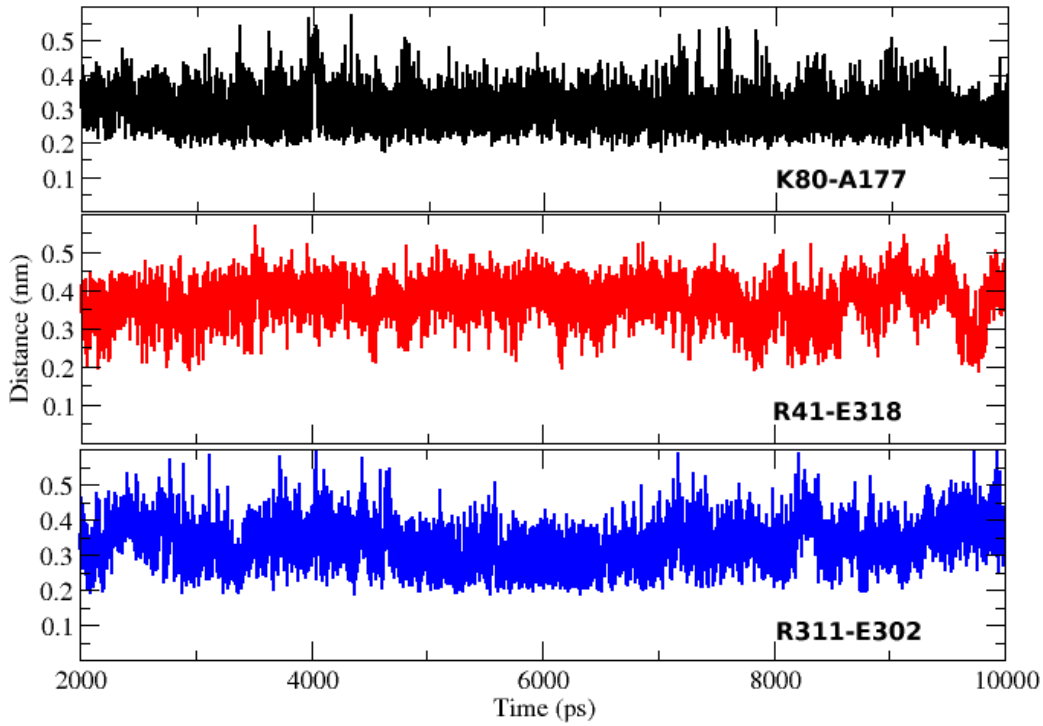

Supplementary Figure S4.

Calculated distances between K80/A177, R41/E318 and R311/E302. The distance between these residues was calculated over the final 8000ps simulation. The initial 2000ps (0-2000ps) have been treated as equilibration step and omitted. The average distances are: K80-A177 (black) = 2.98Å, R41-E318 (red) = 3.72Å, R311-E302 (blue) = 3.32Å.

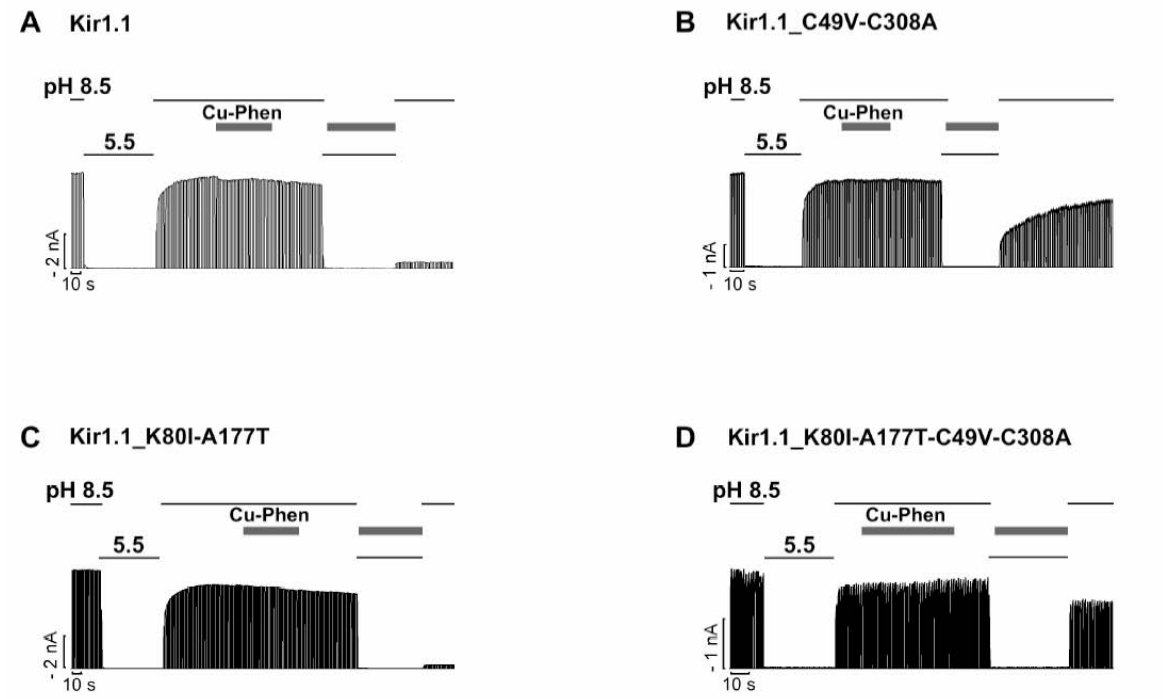

Supplementary Figure S5:

K80I/A177T channels exhibit same state-dependent response to Cu-Phen. In Kir1.1 channels the pH-inhibited state is highly sensitive to cysteine reactive agents, whereas the open state is insensitive. This sensitivity has been attributed to two cysteines; C49 in the N-terminus and C308 in the C-terminus. The regions around these cysteines are thought to move during pH-inhibition, resulting in their exposure and therefore access to modifying agents [Schulte *et al*. 1998]. This figure shows application of 250 µM Cu(II)-1,10, phenanthroline (Cu-Phen) at pH 8.5 and pH 5.5 to (A) wild-type Kir1.1, (B) Kir1.1-C49V/C308A. (C) Kir1.1-K80I/A177T and (D) Kir1.1-K80I/A177T-C49V/C308A channels as indicated; Cu-Phen solutions were gassed with oxygen to enhance the modification by Cu-Phen. Similar results were obtained in n>5 experiments for each mutant respectively. This demonstrates that Cu-Phen produces a state-dependent inhibition of Kir1.1 by modifying channels in the pH-inhibited state, but not in the open state, and that, as expected, the C49A/C308V mutations abolish this effect. Importantly, K80I/A177T mutant channels also exhibit similar state-dependent modification which is abolished by mutation of C49 and C308. Thus implying that the allosteric movements of the cytoplasmic domains which produce pH-inhibition are the same in both wild-type and K80I/A177T mutant channels and argue that that the pH-sensitivity is not restored via an alternative mechanism